



Anodised Titania Nanotubes Prepared in a Glycerol/NaF Electrolyte

D. Regonini^{1,*}, A. Satka², D. W. E. Allsopp³, A. Jaroenworarluck⁴,
R. Stevens¹, and C. R. Bowen¹

¹Materials Research Centre, Department of Mechanical Engineering,
University of Bath, BA2 7AY, UK

²International Laser Center, and Faculty of Electrical Engineering and Information Technology STU,
812 19 Bratislava, Slovakia; Department of Microelectronics, Slovak University of Technology and
International Laser Center, Ilkovicova 3, 812 19 Bratislava, Slovakia

³Department of Electronic and Electrical Engineering, University of Bath, BA2 7AY, UK

⁴MTEC: National Metal and Materials Technology Center, 114 Thailand Science Park, Paholyothin Road,
Klong 1, Klong Luang, Pathumthani 12120, Thailand

This paper discusses the preparation of titania nanotubes by anodisation of Ti in a glycerol-based electrolyte containing 0.5% wt of sodium fluoride (NaF). The influence of anodisation voltage and anodisation time on nanotube wall thickness, diameter and length has been investigated. The results indicate that nanotubes can be formed within a voltage range 10–40 V and that the tubular structure is lost when using a higher voltage. The diameter of the nanotubes is voltage dependent, with the widest tubes being obtained at the highest possible applied voltage of 40 V. An initial voltage ramp which increases at 100 mV/s to the anodisation voltage, rather than an instantaneous step, was observed to stabilise the metal-oxide interface. This enabled the growth of anodic films up to 5.5 μm in length by anodising for approximately 48 h. In the absence of a voltage ramp the films tended to collapse and become detached from the titanium electrode after 15–20 h. Electron microscopy observation suggests that the nanotubes in glycerol develop in a similar way to those produced in water-based media. The nanotubes formed using glycerol also exhibit ripples along the tube wall, although, growing at a slower rate, they are generally smoother than those formed in water.

Keywords: Titanium Dioxide, Titania Nanotubes, Nanoporous Structures, Anodisation, Scansion Electron Microscopy.

RESEARCH ARTICLE

1. INTRODUCTION

Titanium oxide (TiO_2) is of significant interest for its chemical and physical properties,¹ making it suitable for many applications including biomedical,^{2–7} gas-sensing,^{8–14} photo-catalysis,^{15–23} protection of light sensitive materials²⁴ and solar cell devices.^{25–32} Anodisation, sol-gel, hydrothermal, and vapour deposition are the most common techniques employed to generate a variety of nanostructured titanium oxide (titania) morphologies.^{33–35} This paper focuses on the generation of nanotubular titania via anodisation of a metallic titanium electrode, undertaken in a glycerol-based solution containing a small concentration of fluorine ions. A comprehensive review of the growth of anodic titania nanotubes has been recently published by Schmukey and coworkers.³⁶ However, some

aspects of the film growth remain to be clarified. For example, while a number of nanotube formation mechanisms have been proposed,^{37–41} a definitive model that can fully explain the growth and morphology of the nanotubes remains to be published. To form titania nanotubes a small addition of fluorine ions^{42,43} is generally required to initiate the formation of cavities in the anodic structure, although aqueous electrolytes containing chloride ions have also been proven suitable for the growth of random anodised nanotubes.^{44,45} In previous work,⁴⁶ the relatively aggressive nature of water-based electrolytes containing fluorine ions limited the thickness of the nanotubes to less than 2 μm . To reduce the dissolution rate and synthesise thicker layers, recent efforts have focussed on anodic growth of titania nanotubes in organic electrolytes, allowing development of self-organised tubes up to a 1000 μm in length.^{47–54}

*Author to whom correspondence should be addressed.

1.1. Aims of the Work

The aim of this work is to investigate how changes of anodising parameters, such as applied voltage and time, while keeping the electrolyte type and fluorine concentration constant, affect the development of the nanotubes grown in an organic electrolyte. Additional observations related to their growth in an organic electrolyte are made, such as the presence of 'ripples' along the nanotubes and the current-time transients; these are discussed and comparisons made with nanotubes formed in water-based electrolytes.

2. EXPERIMENTAL DETAILS

A commercially pure (99.6%) titanium sheet (0.5 mm thick) was used as an electrode/substrate to be anodised. To complete the cell, a platinum mesh was placed at the cathode to act as a counter-electrode. Prior to anodising, the titanium was ultrasonically cleaned in isopropyl alcohol. A glycerol-based solution containing ~2 wt% water and 0.5 wt% of sodium fluoride (NaF) was used as an electrolyte. The viscosity of the solution, measured with a stress viscometry test (Bholin CS spinning disc rheometer) was ~0.5 Pa·s at room temperature (20 °C). Anodising was performed under potentiostatic conditions, applying a voltage within the range 10–60 V. In some experiments, an initial ramped voltage of 100 mV/s was applied before finally holding the potential at a final pre-determined value between 10 V and 60 V. For example, for an anodisation voltage of 10 V the voltage initially began at 0 V and increased at 100 mV/s for 100 s to 10 V and was then maintained constant at 10 V for a specific dwell time. The dwell time at the final anodisation voltage was varied from a minimum of 4 h to a maximum of 100 h. The electrolyte was slightly stirred during the experiment. The electrolyte type and temperature (20 °C) were maintained constant for all the experiments. The anodised specimens were examined in a Scanning Electron Microscope (SEM), (JEOL JSM6480LV), and a Field Emission SEM (FE SEM LEO 1550 with in-lens secondary electron detector) for higher resolution. Nanotube length (L), tube diameter (D) and wall thickness (W) were estimated from electron microscopy observations. Three specimens were prepared for each anodisation condition to evaluate nanotube dimensions.

3. RESULTS AND DISCUSSION

A summary of the results for the nanotube length for the various anodisation voltages and times is shown in Table I; which also identifies the type of structure obtained (nanotubes or random porosity).

3.1. Application of Voltage Ramp

For all the data presented in Table I, a ramp rate of 100 mV/s was applied before holding the voltage constant

Table I. Type and length (L) of the anodic layers obtained at different voltages and anodising times in a glycerol/NaF solution.

Anodising condition (voltage/time) (V)	4 h (μm)	24 h (μm)	48 h (μm)	100 h (μm)	Anodised structure
10	0.5	0.5	0.5	—	Nanotubes
20	1	1.5–2	4	<4	Nanotubes
30	1.5	2–3	5.5	<5.5	Nanotubes
40	1	2	4	—	Nanotubes
60	1	1	1	—	Random pores

at 10, 20, 30, 40 or 60 V. In the absence of a voltage ramp, the films produced in the organic electrolyte were observed to detach from the titanium electrode after anodising for 15–20 h. From previously reported observations on nanotubes prepared in a water-based electrolyte,⁴⁶ the application of an initial voltage ramp ensured the development of a well-interconnected network of cavities from the early stages of the anodisation process. This is thought to help release stress at the metal/metal oxide (M/MO) interface and aid retention of the titania film on the titanium substrate. In addition, when applying an instantaneous voltage step (i.e., no ramp), the migration of Ti^{4+} ions from the metal to the oxide/electrolyte interface through the anodic layer is rapid since the electric field across the oxide (voltage/thickness) is relatively high during the early stages of anodisation. This generates vacancies and further stress into the structure.⁴¹

3.2. Type of Nanostructure as a Function of the Applied Voltage

The applied voltage determined the type of anodic structure produced. Anodisation at the highest voltage of 60 V did not lead to a nanotubular morphology and the as-formed film, Figure 1(a), exhibited a sponge-like structure with the presence of randomly dispersed nanopores. Nanotube structures were formed when anodising within a voltage range of 10–40 V (Table I) and SEM images showing the typical morphology of the nanotubes can be seen in Fig. 1(b–d). The mouth (upper part) of the nanotubes, Figure 1(b), is covered by a dense barrier type layer, in which SEM-energy dispersive spectrometry (EDS) showed the presence of oxygen and titanium. It is likely that the top layer is freshly formed titanium dioxide, which has not undergone etching by the fluorine ions and therefore does not have pores. This obstructing barrier layer can be removed either by washing the specimen in a dilute solution of hydrofluoric acid (1 vol.%), or by ultrasonic cleaning in isopropyl alcohol.⁴⁸ Cleaning in hydrofluoric acid, Figure 1(c), cannot be extended to more than few seconds since it is rather aggressive and weakens the anodic film at the M/MO interface, facilitating its detachment from the substrate. However the use of isopropyl alcohol leads to better cleaning without damaging the structure, Figure 1(d). The need to clear the upper mouth of the

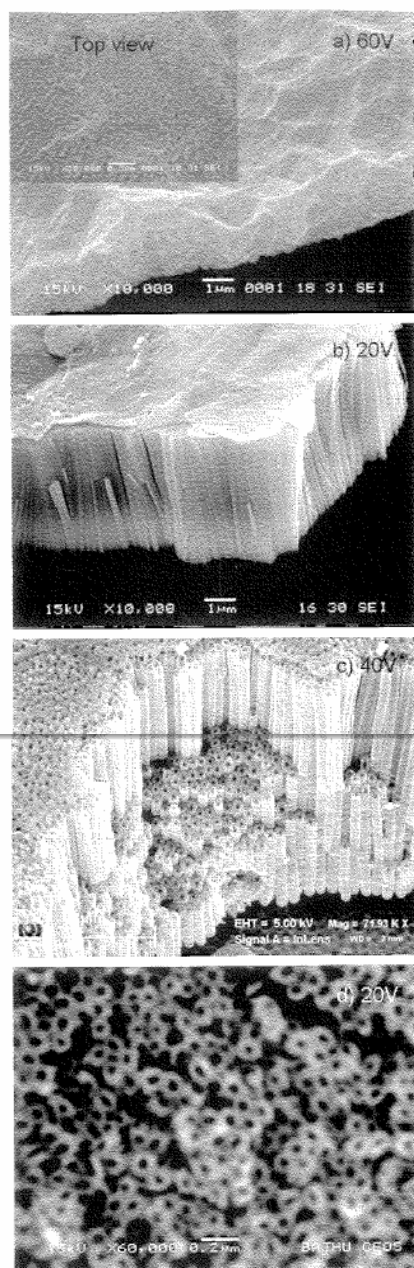


Fig. 1. SEM images of anodic structures prepared in glycerol/NaF: porous layer at 60 V (a), upper view of the nanotubes (20 V) before cleaning (b), after the cleaning procedure in hydrofluoric acid (c) and isopropyl alcohol (d) to remove the top layer which covers the mouth of the tubes.

nanotubes from any precipitates or unwanted barrier layer detritus is of particular importance for characterisation and technological application of the nanotubes, for example in dye-sensitised solar cell devices.⁵⁵

3.3. The Effect of the Applied Voltage and Time on Nanotube Length (L)

It is also of interest to examine the influence of the applied voltage on the final thickness of the layer, since the primary aim in using the organic electrolyte is to reduce the titania dissolution rate and create longer nanotubes. When anodising at 10 V, the oxidation process ceases at an early stage, resulting in a relatively short tubes, just 0.5 μm long. This implies that the length of the nanotubes quickly becomes independent of time and remains approximately 0.5 μm even by extending the anodising time up to 48 hr or longer (see Table I). However, 4 μm and 5.5 μm long

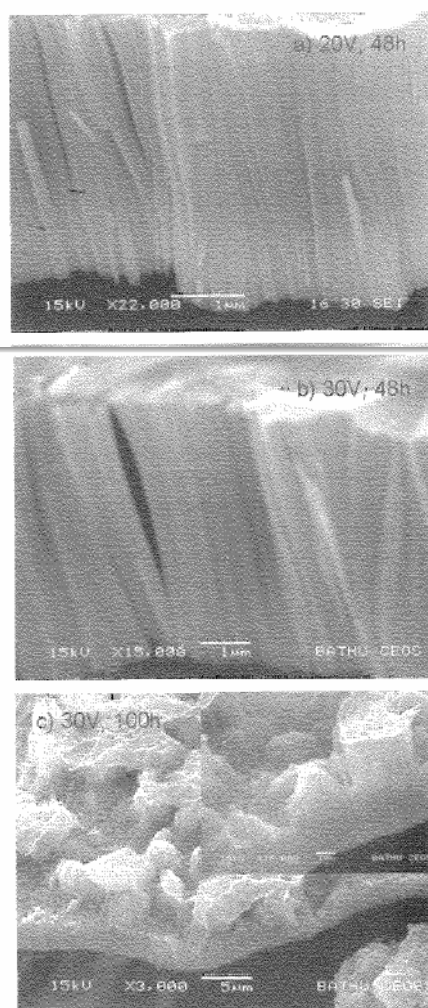
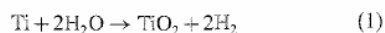


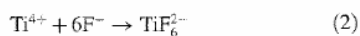
Fig. 2. SEM images of a 4 μm (a) and 5.5 μm (b) long nanotube layers obtained at 20 V and 30 V respectively after anodising the specimen for 48 h. Further extension of the anodising time does not lead to thicker films, because the structure partially collapses (c).

tubes can be grown by increasing the voltage up to 20 V, Figure 2(a), and 30 V, Figure 2(b) respectively. The contributions provided by the use of higher anodisation voltages can be separated in terms of field assisted oxidation (Eq. (1)) and dissolution (Eq. (2)):

Field-assisted oxidation:

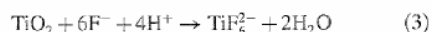


Field-assisted dissolution:



In addition there is chemical dissolution as a result of the presence of fluorine ions (Eq. (3)):

Chemical dissolution:



An increase in the field-assisted oxidation implies enhanced migration of ions such as Ti^{4+} , O^{2-} and OH^- through the anodic titania film. This helps to overcome the resistance developed at the M/MO interface as a result of the barrier layer developing at the base of the tubes and along the tube wall. This maintains an active oxidation process for a longer period and generates thicker titania films. The nanotube length increases until the oxidation rate (Eq. (1)) equals the dissolution rate of the upper surface of the tubes (Eq. (3)). After this critical point, the nanotube length is independent of time: In addition to the enhanced oxidation at higher anodisation voltages, it is necessary to consider the effect of the initial voltage ramp rate of 100 mV/s, which maintains a relatively thin barrier layer and contributes to optimise current flow. From Table I it can be seen that the nanotube length begins to decrease when anodising at a voltage of 40 V or more. It is possible to explain this behaviour assuming that the field-assisted dissolution (Eq. (2)) competes with the oxidation process (Eq. (1)). It should also be noted that the maximum nanotube length is achieved by anodising for a period of 48 h and the same trend is observed at 20 and 30 V. Extending the anodisation time to 100 h did not lead to longer nanotubes but actually results in a decrease compared to the length achieved at 48 hr (see Table I). One would expect a constant length after having achieved equilibrium between oxidation and dissolution. A decrease in tube length at extended anodisation times has also been observed by Paulose et al.⁴⁸ SEM observations indicated that the decrease in film thickness for times in excess of 48 h was due to region of the anodic oxide detaching from the electrode, removing sections of the titania film formed during the first 48 h of anodisation, Figure 2(c).

3.4. The Effect of the Applied Voltage on the Wall Thickness and the Diameter of the Tubes

The correlation between the tube diameter and the applied voltage has been previously reported for films grown in

Table II. Different nanotube diameter (D) and wall thickness (W) obtained by varying the applied voltage.

Applied voltage (V)	Diameter (D) (nm)	Wall thickness (W) (nm)
10	19 ± 2	11 ± 1
20	34 ± 8	16 ± 3
30	63 ± 5	19 ± 2
40	75 ± 5	24 ± 2

water-based media.⁵⁶ The results for the organic electrolyte obtained within the anodisation range of 10–40 V (the voltage range which formed nanotubes) are summarised in Table II. Internal diameter (D) and walls thickness (W) values have been measured from a combination of electro-microscopy images (typically 30–50 nanotubes). Examples of SEM images used to calculate D and W can be seen in Figures 3(a–b). When anodising in a glycerol based electrolyte the diameter of the nanotubes formed is dependent on the applied voltage, with larger diameter tubes being obtained at the higher anodisation voltages. Table II also indicates that the anodisation voltage also affects the wall thickness; with thicker walls developed by increasing the voltage. On increasing the voltage from 10 to 40 V, the diameter varies from a minimum of 19 ± 2 nm to a maximum of 75 ± 5 nm and the wall thickness from 11 ± 1 nm up to 24 ± 2 nm (Table II). Both the diameter and wall

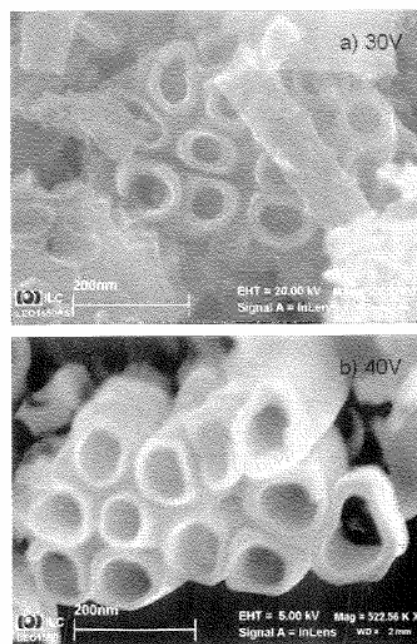


Fig. 3. SEM images of nanotubes prepared in glycerol/NaF applying different voltages: 30 V (a) and 40 V (b). The higher the voltage, the larger the nanotube diameter and wall thickness.

thickness increments can be related to the enhanced oxidation associated with the increased voltage. A higher voltage extends the migration distance of ions and maintains an active oxidation process through thicker layers, leading to thicker walls. For the same reason the developing oxide nanoparticles extend to a larger size and, once properly etched, produce channels of a larger diameter than those prepared at lower voltage. A larger diameter also suggests the dissolution rate increases with voltage and supports the observations that longer tubes were not necessarily formed at the highest anodisation voltage (Table I). For example, at 40 V, where chemical dissolution is aided by field assisted dissolution the nanotubes are wider (higher migration of ions), but shorter (higher dissolution) than those obtained at 30 V.

3.5. The Formation of Ripples Along the Tubes Wall

It has been commonly reported^{53,54} that one clear distinction between tubes grown in aqueous and organic electrolytes is that water based nanotubes exhibit 'ripples' along the nanotube walls, resulting in a non-homogeneous tube wall thickness. Organic electrolytes tend to form smooth tube walls with a constant tube wall thickness. Ripples along the wall of tubes grown in aqueous electrolytes have been associated with pH bursts, a local temporary acidification which occurs when the oxide forms and locally increases the oxide dissolution rate.⁴⁷ However, in this work the presence of 'ripples' (which are identified as oxide rings) are also observed in nanotubes prepared using an electrolyte based on 98% glycerol. When using water based electrolytes, we suggested the rings are nanoparticles of oxide that form at different stages and link up together, to optimise the passage of current.⁴⁰ The observations of ripples in Figure 4(a) (and inset) suggest that the nanotubes in glycerol develop in a similar way to those produced in water-based media. Nanotubes are often smooth when formed in organic media due to the fact that (almost) anhydrous electrolytes are used⁴⁷⁻⁵⁴ and the only water to support the reaction was that adsorbed from atmospheric moisture. In this work the water content of the electrolyte was ~2 wt% and evolution of gas at the anode was observed, particularly during the early stages of the anodisation process. Ripples along the tube length may be the result of oxygen evolution due to electrolysis of water at the anode, which can only occur providing sufficient water is present in the electrolyte and the barrier layer oxide at the M/MO interface is relatively thin and allows electrons to pass through the oxide. Recent work by Raya et al.⁵⁷ support these observations since they investigated the role of water in the anodisation process and concluded a minimum amount of water (0.18 wt%) was needed to promote oxidation and ensure nanotube growth. They also noted that when the water content exceeded 0.5 wt%, the tubes exhibited ripples. Occasionally, the nanotubes

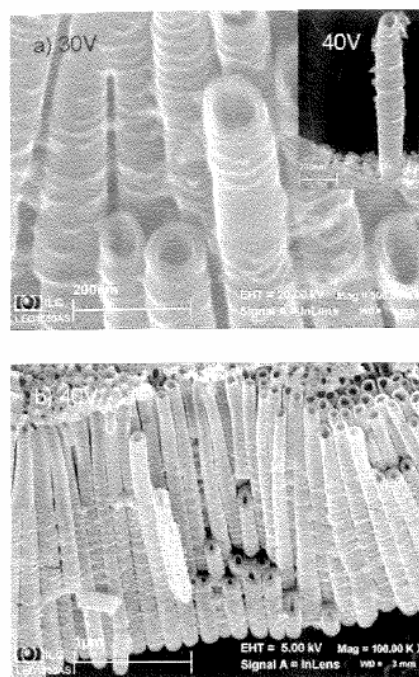


Fig. 4. SEM cross sectional views of the tubes highlighting the presence of ripples (rings) along the tubular structure (a); with a single standing tube in the inset. Partially smooth profile where changes in morphology can be attributed to the higher viscosity of the solution, which may facilitate relaxation of the structure initially formed (b).

prepared in this work are observed to be completely or partially smooth, as in Figure 4(b). This intermediate situation is never observed in water-based electrolytes. Since the oxidation process is much slower in glycerol, the longer timescales may well enable relaxation of the nanostructure ultimately developing a smooth surface structure to the tube.

3.6. The Current Transient Registered During Anodisation in Glycerol/NaF

The current transients observed during the anodisation of titanium in glycerol/NaF solution at a variety of voltages are shown in Figure 5. The curves show the profile obtained after having applied an initial ramp rate of 100 mV/s to achieve a final constant voltage within the range 10–60 V. Higher voltages corresponds to higher currents. The curves are typical of a porous/tubular layer and the shape is identical to those we obtained in water-based solutions.⁴⁶ The only difference is the timescale, since the process in organic media is much slower due to the higher viscosity and lower conductivity of the electrolyte and hence the different stages of anodisation are well separated in three different stages. At first the current decreases

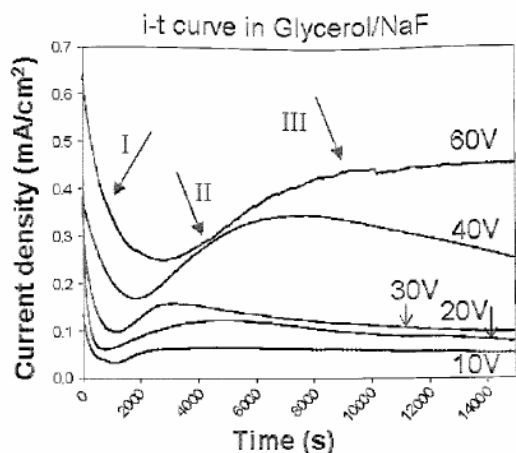


Fig. 5. Current-transients observed during the anodisation of titanium at different voltages in glycerol/NaF. Curves were registered at constant voltage, after ramping from 0 V to its final value (10–60 V) at 100 mV/s.

indicating thickening of the barrier layer is dominant with respect to the generation of cavities and pores (stage I). The current then rises once cavities and pores linked up to create channels where current flow is optimised, balancing the thickening of the anodic layer (stage II). Finally current becomes constant or decreases slightly (stage III). The oxidation process ceases once the migration of ions through the barrier layer beneath the structure and through the anodic layer is reduced to a point where it is equal to the dissolution rate of the oxide at the top of the tubes. Unlike the current transient recorded in water, no current oscillations are observed, apart from the experiments performed at 60 V.

4. CONCLUSIONS

This paper has examined how changes of anodising parameters, such as applied voltage and time, while keeping the electrolyte type and fluorine concentrations constant, affect the development of the nanotubes grown in an organic (glycerol-based) electrolyte containing 0.5 wt% of sodium fluoride (NaF). The use of an organic electrolyte allows the growth of longer TiO₂ nanotube layers, compared to water based electrolyte. Titania nanotubes can be formed within a voltage range 10–40 V and the nanotubular structure is lost when a higher voltage is used. The nanotube diameter is voltage dependent, with the widest diameter tubes being formed at 40 V. An initial voltage ramp (100 mV/s) to the anodisation voltage, rather than an instantaneous step was observed to stabilise the metal-oxide interface and enables the growth of anodic films up to 5.5 μm in length by anodising for approximately 48 h. Longer anodisation periods (100 h) lead to a decrease in anodic film thickness. In the absence of a voltage ramp, the films tended to collapse

and become detached from the titanium electrode after 15–20 h. Nanotubes formed in glycerol have been shown to exhibit ripples along the tubes walls, although they are generally smoother than the surfaces of tubes formed in water. The ripples are thought to be a consequence of the presence of water (~2 wt%) within the electrolyte undergoing electrolysis to form oxygen. In terms of the current time transients, the curve is typical of a porous/tubular layer and the shape is identical to the one obtained in water-based solutions. SEM observations indicate the formation mechanisms in glycerol and water appear to be identical. The major difference is the timescale employed for growth, the anodisation process in organic media being slower due to the higher viscosity and lower conductivity of the electrolyte.

Acknowledgments: The University of Bath, The Royal Academy of Engineering and The Worshipful Company of Armourers and Brasiers and MTEC are acknowledged for kindly supporting this research project.

References and Notes

- U. Diebold, *Surf. Sci. Rep.* 48, 53 (2003).
- X. Zhu, K. H. Kim, and Y. Jeong, *Biomaterials* 22, 2199 (2001).
- B. C. Yang, M. Uchida, H. M. Kim, X. D. Zhang, and T. Kokubo, *Biomaterials* 25, 1003 (2004).
- S. H. Oh, R. R. Finões, C. Daraio, L. H. Cen, and S. Jin, *Biomaterials* 26, 4938 (2005).
- T. Kokubo, T. Matsushita, and H. Takadama, *J. Eur. Ceram. Soc.* 27, 1553 (2007).
- K. C. Popata, L. Leonib, C. A. Grimes, and T. A. Desai, *Biomaterials* 28, 3188 (2007).
- K. C. Popata, M. Eltgroth, T. J. LaTempa, C. A. Grimes, and T. A. Desai, *Biomaterials* 28, 4880 (2007).
- K. Zakrzewska, *Vacuum* 74, 335 (2004).
- S. Akbar, P. Dutta, and C. Lee, *Int. J. Appl. Ceram. Technol.* 3, 302 (2006).
- G. K. Mor, M. A. Carvalho, M. V. Pishko, and C. A. Grimes, *J. Mat. Res.* 19, 628 (2004).
- O. K. Varghese and C. A. Grimes, *J. Nanosci. Nanotechnol.* 3, 277 (2003).
- O. K. Varghese, D. Gong, M. Paulose, K. G. Ong, and C. A. Grimes, *Sensors and Actuators B: Chemical* 93, 338 (2003).
- O. K. Varghese, D. Gong, M. Paulose, K. G. Ong, E. C. Dickey, and C. A. Grimes, *Adv. Mater.* 15, 624 (2003).
- M. Paulose, O. K. Varghese, G. K. Mor, C. A. Grimes, and K. G. Ong, *Nanotechnology* 17, 398 (2006).
- M. A. Fox and M. T. Dulay, *Chem. Rev.* 93, 341 (1993).
- M. R. Hoffmann, S. T. Martin, W. Choi, and D. W. Bahnemann, *Chem. Rev.* 95, 69 (1995).
- A. Mills, G. Hill, S. Bhopal, I. P. Parkin, and S. A. O'Neill, *J. Photochem. and Photobiol. A: Chem.* 160, 185 (2003).
- G. K. Mor, K. Shankar, O. K. Varghese, and C. A. Grimes, *J. Mat. Res.* 19, 2989 (2004).
- B. M. Reddy, I. Ganesh, and A. Khan, *J. Molecular Cat. A: Chem.* 223, 295 (2004).
- H. D. Jang, S.-K Kim, and S.-J Kim, *J. Nanoparticle Res.* 3, 141 (2001).
- T. Minabe, D. A. Tryk, P. Sawunyama, Y. Kikuchi, K. Hashimoto, and A. Fujishima, *J. Photochem. and Photobiol. A: Chem.* 137, 53 (2000).

22. G. K. Mor, K. Shankar, M. Paulose, O. K. Varghese, and C. A. Grimes, *Nano Lett.* 5, 191 (2005).
23. A. Fujishima, T. N. Rao, and D. A. Tryk, *J. Photochem. and Photobiol. C: Rev.* 1, 1 (2000).
24. M. Zayat, P. G. Parejo, and D. Levy, *Chem. Soc. Rev.* 36, 1270 (2007).
25. M. Grätzel, *Nature* 414, 338 (2001).
26. M. Grätzel, *J. Photochem. and Photobiol. C: Photochem. Rev.* 4, 145 (2003).
27. Y. Xie, L. M. Zhou, and H. Huang, *Mater. Letters* 60, 3558 (2006).
28. G. K. Mor, O. K. Varghese, M. Paulose, K. Shankar, and C. A. Grimes, *Sol. Energy Mater. Sol. Cells* 90, 2011 (2006).
29. J. H. Park, S. Kim, and A. J. Bard, *Nano Lett.* 6, 24 (2006).
30. J. M. Macak, H. Tsuchiya, A. Ghicov, and P. Schmuki, *Electrochem. Comm.* 7, 1133 (2005).
31. G. K. Mor, K. Shankar, M. Paulose, O. K. Varghese, and C. A. Grimes, *Nano Lett.* 6, 215 (2006).
32. N.-G. Park, J. Van de Lagemaat, and A. J. Frank, *J. Phys. Chem. B* 104, 8989 (2000).
33. X. Chen and S. S. Mao, *J. Nanosci. Nanotechnol.* 6, 906 (2006).
34. X. Chen and S. S. Mao, *Chem. Rev.* 107, 2891 (2007).
35. D. V. Bavykin, J. M. Friedrich, and F. C. Walsh, *Adv. Mater.* 18, 2807 (2006).
36. J. M. Macak, H. Tsuchiya, A. Ghicov, K. Yasuda, R. Hahn, S. Bauer, and P. Schmuki, *Curr. Opin. Solid State Mater. Sci.* 11, 3 (2007).
37. L. V. Taveira, J. M. Macak, H. Tsuchiya, L. F. P. Dick, and P. Schmuki, *J. Electrochem. Soc.* 152, B405 (2005).
38. G. K. Mor, O. K. Varghese, M. Paulose, N. Mukherjee, and C. A. Grimes, *J. Mat. Res.* 18, 2588 (2003).
39. J. M. Macak, H. Tsuchiya, and P. Schmuki, *Angew. Chem. Int. Ed.* 44, 2100 (2005).
40. A. Jaroenworarluck, D. Regonini, C. R. Bowen, R. Stevens, and D. Aillsopp, *J. Mat. Sci.* 42, 6729 (2007).
41. K. Yasuda, J. M. Macak, S. Berger, A. Ghicov, and P. Schmuki, *J. Electrochem. Soc.* 154, C472 (2007).
42. V. Zwillling, E. Darque-Ceretti, A. Boutry-Forveille, D. David, M. Y. Perrin, and M. Aucouturier, *Surf. Interface Anal.* 27, 629 (1999).
43. D. Gong, C. A. Grimes, O. K. Varghese, W. Hu, R. S. Singh, Z. Chen, and E. C. Dickey, *J. Mat. Res.* 16, 3331 (2001).
44. R. Hahn, J. M. Macak, and P. Schmuki, *Electrochem. Comm.* 9, 947 (2007).
45. N. K. Aillam and C. A. Grimes, *J. Phys. Chem. C* 111, 13028 (2007).
46. D. Regonini, C. R. Bowen, R. Stevens, D. Aillsopp, and A. Jaroenworarluck, *Phys. Stat. Sol. (a)* 204, 1814 (2007).
47. J. M. Macak, H. Tsuchiya, L. Taveira, S. Aldabergerova, and P. Schmuki, *Angew. Chem. Int. Ed.* 44, 7463 (2005).
48. M. Paulose, K. Shankar, S. Yoriya, H. E. Prakasham, O. K. Varghese, G. K. Mor, T. A. Latempa, A. Fitzgerald, and C. A. Grimes, *J. Phys. Chem. B* 110, 16179 (2006).
49. K. Shankar, G. K. Mor, A. Fitzgerald, and C. A. Grimes, *J. Phys. Chem. C* 111, 21 (2007).
50. H. E. Prakasham, K. Shankar, M. Paulose, O. K. Varghese, and C. A. Grimes, *J. Phys. Chem. C* 111, 7235 (2007).
51. C. A. Grimes, *J. Mat. Chem.* 17, 1451 (2007).
52. M. Paulose, H. E. Prakasham, O. K. Varghese, L. Peng, K. C. Popat, G. K. Mor, T. A. Desai, and C. A. Grimes, *J. Phys. Chem. C* 111, 14992 (2007).
53. S. P. Albu, A. Ghicov, J. M. Macak, and P. Schmuki, *Phys. Stat. Sol. (RRL)* 1, R65 (2007).
54. J. M. Macak, S. P. Albu, and P. Schmuki, *Phys. Stat. Sol. (RRL)* 1, 181 (2007).
55. K. Zhu, N. R. Neale, A. Miedaner, and A. J. Frank, *Nanoletters* 7, 69 (2007).
56. Q. Cai, M. Paulose, O. K. Varghese, and C. A. Grimes, *J. Mater. Res.* 20, 230 (2005).
57. K. S. Raja, T. Gandhi, and M. Misra, *Electrochem. Comm.* 9, 1069 (2007).

Received: 10 January 2008. Accepted: 10 March 2008.